

1 This is a non-peer reviewed preprint submitted to EarthArXiv.

2 **Listening to Manchester: Using citizen science Raspberry Shake seismometers to quantify road**
3 **traffic**

4 A. David Healy^{1, 2*}

5

6 ¹Department of Geology & Geophysics, School of Geosciences, University of Aberdeen, Aberdeen,

7 United Kingdom

8 ²Visiting Academic at Department of Earth & Environmental Sciences, University of Manchester,

9 United Kingdom

10 *Corresponding author: d.healy@abdn.ac.uk

11

12 **Author ORCID**

13 A. David Healy: 0000-0003-2685-1498

14

15 **Author contributions**

16 Conceptualization: A. David Healy

17 Formal Analysis: A. David Healy

18 Software: C. David Healy

19 Writing – original draft: A. David Healy

20 Writing – review & editing: A. David Healy

21

22 **Abstract**

23 Road traffic is a major contributor to greenhouse gases in our cities. This study has been designed

24 to test whether low-cost citizen science seismometers (Raspberry Shakes) can be used to quantify

25 temporal and spatial variations in road traffic. I used a network of seismometers installed around

26 Greater Manchester to record signals in the frequency range 1-50 Hz. Data were processed using

27 the open source ObsPy package. Results show that daily variations in seismic noise in this
28 frequency range correlate directly with vehicle counts from open access traffic cameras installed
29 nearby. In addition, a simple peak-counting method can be applied to the seismometer recordings
30 to measure individual passing vehicles, which correlate directly with in-person traffic counts. Two
31 seismometers were installed close to a School Streets pilot project to test if traffic volumes
32 increased just outside the road closure section. Results to data show no increase in seismic
33 vibrations attributable to road traffic, over 6 road closure days. The combination of low unit cost
34 and transparent (i.e., open) data from these seismometers makes them a useful tool to
35 simultaneously quantify anthropogenic noise – including road traffic – and share the results with
36 the wider public.

37

38 **Non-technical summary**

39 Road traffic in urban areas contributes significantly to the amount of carbon dioxide and
40 particulates in the atmosphere. It is important therefore to accurately measure and quantify road
41 traffic and how it varies over space and time – for example, in response to policy changes.
42 Camera-based systems for counting vehicles can be expensive and can generate concerns in the
43 public over anonymity. In this study, I used low-cost seismometers – more commonly used to
44 record earthquakes and volcanic eruptions – to quantify variations in road traffic around Greater
45 Manchester. By comparing the data from the newly installed seismometers with data from
46 existing digital traffic cameras, I show that the seismometers can accurately count vehicles across
47 a range of locations from city centre to more rural communities. All of the data and code used in
48 this study is publicly available – a key requirement for including the wider community in discussion
49 and debate around the changes needed to tackle the climate emergency.

50

51 **1. Introduction**

52 *1.1 Background & Rationale*

53 The urban environment generates seismological vibrations, which can be considered as either
54 signal or noise. Depending on the location of a specific city, the spectral content of these
55 vibrations is of interest to civil engineers, city planners and those responsible for quantifying
56 earthquake or volcano hazards (refs). In general, the dominant source of these vibrations in urban
57 areas is anthropogenic – chiefly from transport and industrial activity. It is increasingly important
58 to characterise and quantify the amplitude and spectral signature of these non-natural sources, in
59 part to better understand their effects on, and relationship to, generally lower frequency signals
60 from natural sources.

61 We are now in a climate emergency, with the concentration of greenhouse gases (GHG) in
62 the atmosphere rising and driving global warming (IPCC, 2021). The key component in GHG is
63 carbon dioxide (CO₂) which is generated by the burning of fossil fuels. In the Greater Manchester
64 (GM) area, the largest single contributor to atmospheric CO₂ is transport (38%; Department for
65 Business, Energy and Industrial Strategy, 2021). It is important to note that the traffic volume data
66 used in these published reports are heavily dependent on estimates and extrapolations, with very
67 few direct measurements. The Listen to Manchester project has been designed to address this
68 issue by using low cost citizen science seismometers to quantify traffic patterns across the GM
69 area (see Figure 1). Greater Manchester is a large urban and suburban area in NW England (UK),
70 with a population estimated at 2.8M (census of 2021; Office for National Statistics, 2023). The area
71 is served by a range of transport networks including trains, buses, and trams, and has a high road
72 traffic density. One key reason for locating this project in the GM area is the simultaneous
73 availability of public data from traffic cameras and other sensors in the manchester-i network
74 managed by the Manchester Urban Observatory. These open data allow for direct comparisons
75 and calibrations of data measured on the seismometer and their dissemination to the wider
76 public.

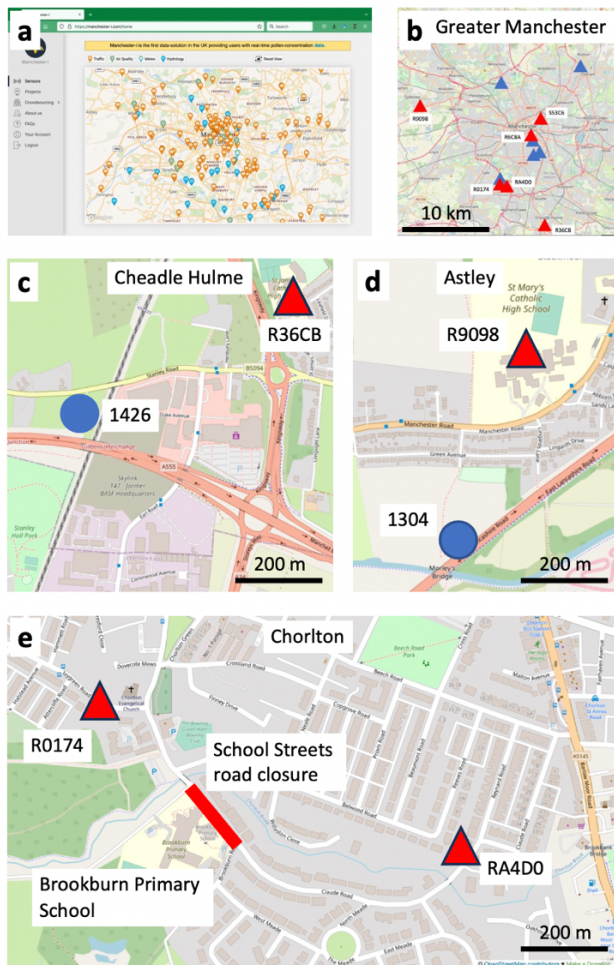
77 The bedrock of the Greater Manchester area comprises Upper Palaeozoic and Mesozoic
78 sedimentary rocks, including faulted and folded Carboniferous Coal Measures unconformably
79 overlain by faulted Permo-Triassic sandstones and conglomerates of the Cheshire Basin. These
80 rocks are overlain by Quaternary alluvium and river gravels in the Mersey and Irwell valleys (Plant
81 et al., 1999). Natural seismic activity is not unknown, with a well-studied swarm of over 100
82 earthquakes in late 2002 beneath the city centre, up to magnitude M_L 3.9. Hypocenters of these
83 events were located to pre-existing faults 2-3 km beneath the city, and 6 focal mechanisms show
84 strike-slip fault movements (Walker et al., 2003).

85

Station	Location (latitude, longitude)	Model (RS prefix = Raspberry Shake)	Comments on site
<i>Stations used in this study</i>			
R0174	53.4324, -2.2836	RS1D	House
R36CB	53.3604, -2.1889	RS1D	Secondary school
R6C8A	53.4685, -2.2249	RS1D	University
R9098	53.4865, -2.4533	RS3D	Secondary school
RA4D0	53.4324, -2.2684	RS1D	House
S53C6	53.4775, -2.1798	RS3D	College
<i>Other stations in Listen to Manchester network</i>			
R1770	53.4324, -2.2684	RS1D	Primary school
R3FEA	53.4414, -2.2689	RS1D	Primary school

R34A7	53.4414, -2.2086	RS3D	Secondary school
RAEED	53.4595, -2.2247	RS1D	University
R4DD7	53.4414, -2.2084	RS3D	Botanical garden
R0DB4	53.5315, -2.1072	RS3D	College
R9E71	53.5135, -2.2729	RS1D	House
RD9D6	53.2613, -2.1542	RS3D	Secondary school
R6055	53.4144, -4.3231	RS1D	Visitor centre
R6AAD	52.8649, -4.5525	RS3D	Secondary school
R9EF0	52.9279, -4.5141	RS1D	Community hall
RC8D6	52.8198, -4.5025	RS1D	Community hall
RE28A	53.2252, -4.1534	RS3D	University
<i>Nearest BGS broadband station</i>			
LBWR	53.402, -1.725	CMG-3T	(no data)

86 **Table 1.** List of seismometers installed for the Listen to Manchester project, and details of the nearest reference
87 British Geological Survey (BGS) broadband seismometer (LBWR) at Ladybower reservoir in the Peak District.



89

90 **Figure 1.** Maps of Greater Manchester (GM) showing locations of devices. **a)** Screenshot of manchester-i
 91 repository from the Manchester Urban Observatory, showing the distribution of traffic cameras and other
 92 environmental sensors across the GM area. **b)** Map of GM showing the Raspberry Shakes installed to date (May
 93 2023) in the Listen to Manchester project. Stations used in this study shown by red triangles and other stations
 94 as blue triangles. **c)** Map of Cheadle Hulme (south Manchester) showing proximity of Drakewell traffic camera
 95 1426 to seismometer station R36CB. **d)** Map of Astley (west Manchester) showing proximity of Drakewell traffic
 96 camera 1304 to seismometer R9098. **e)** Map of Chorlton (south Manchester) showing locations of seismometers
 97 installed to monitor local traffic around a school as part of the School Streets pilot.

98

99 *1.2 Previous work*

100 Previous work has quantified seismological data in urban environments using broadband
 101 seismometers including: trains, aircraft and cars around Long Beach (California, USA; Riahi &
 102 Gerstoft, 2015); crowds at rugby matches and the trains used to transport people there in

103 Auckland (New Zealand; Boese et al., 2015); subway (underground) trains, football matches and
104 music concerts in Barcelona (Spain; Diaz et al., YYYY); transport in London (UK; Green et al., 2017);
105 and crowd responses to football matches when Leicester City won the Premier League in
106 2015/2016 (Leicester, UK; Denton et al., 2018). A pronounced global decrease in urban
107 anthropogenic ‘noise’ was recorded – in part on Raspberry Shake seismometers – during the
108 COVID-19 epidemic (Lecocq et al., 2019). Data from a network of Raspberry Shake seismometers
109 installed around an active geothermal drilling project in rural Cornwall has recently shown that
110 these devices can provide useful preliminary assessment of ground motion from induced
111 seismicity (Holmgren & Werner, 2021).

112

113 *1.3 Specific scope of this paper*

114 In this paper, I used a network of Raspberry Shake seismometers to measure and quantify road
115 traffic over a wide urban and suburban area around Greater Manchester. Seismological vibrations
116 are compared directly to digital traffic count data from the previously installed traffic camera
117 network. I compare the spectral response of locally installed seismometers to time-series data
118 from the nearest traffic cameras, and determine the optimum frequencies to characterise the
119 local traffic volume. The key questions addressed are:

- 120 • What part of the spectral response at each seismometer is due to road traffic? And
- 121 • If we can define and isolate that response, can we use the seismometer signals to directly
122 measure traffic volumes in the absence of specialised road traffic cameras?

123 Data are also presented for the example of a local road closure programme around a primary
124 school in South Manchester, part of the School Streets road closure pilot scheme at Brookburn
125 Primary School, Chorlton to encourage active travel.

126

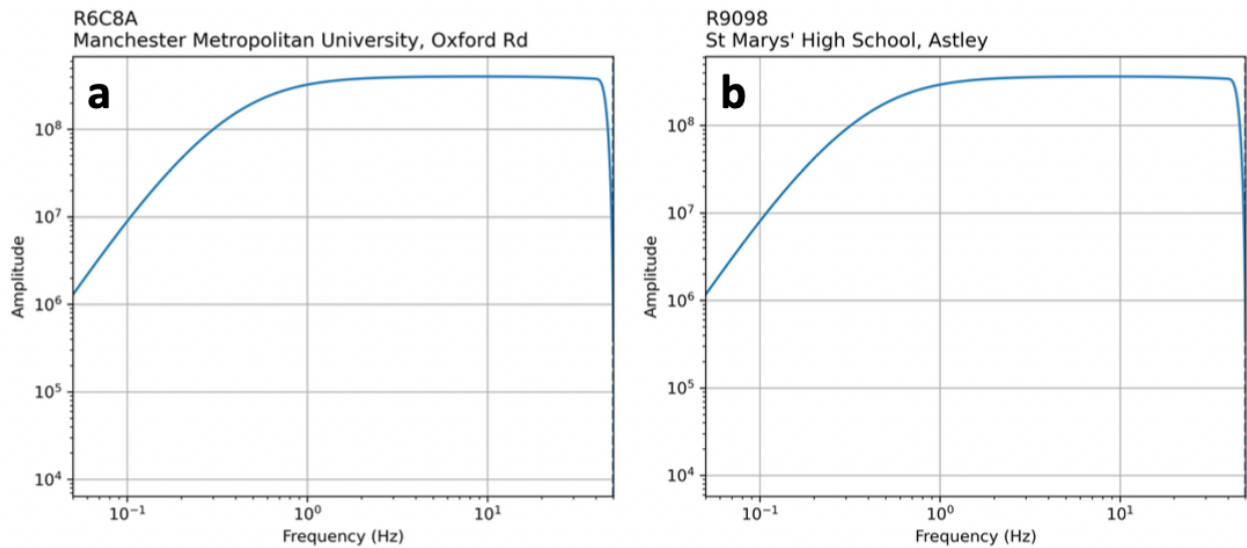
127 **2. Methods**

128 A total of nineteen Raspberry Shake 1- and 3- component seismometers (models RS1D and RS3D
129 respectively) have been deployed to date in buildings across Greater Manchester, including four in
130 North Wales, for the Listen to Manchester project (see Figure 1). Sites include schools,
131 universities, community halls and private domestic houses. Wherever possible, the devices were
132 installed on concrete floors in the lowest level of the buildings, and situated away from heating or
133 air conditioning units and areas of heavy pedestrian traffic. All devices are set to sample at 100
134 samples per second. Only vertical components are used in this study, as several of the deployed
135 devices were 1D (i.e., a single vertical geophone) only. The six specific devices used in this paper
136 are shown in red in Figure 1.

137 Pre-processing of the seismometer data included removing the instrument response from
138 each station, and the application of a high pass filter set at 1 Hz. Power Spectral Density (PSD) was
139 calculated with a Fourier transform method through the open source ObsPy PPSD object class,
140 using half-hour segments and smoothed over one octave bands and one-eighth octave intervals
141 (the same technique used in Green et al., 2017). PSD values are plotted and reported in decibel
142 (dB) units with respect to acceleration power (i.e., $\text{m}^2/\text{s}^4/\text{Hz}$). All times are plotted and reported
143 as either UTC or British Summer Time (BST = UTC + 1 hour), depending on the time of year.

144 Examples of the frequency response of two stations used in this study are shown in Figure
145 2. For both RS1D and RS3D devices, the flat part of the response lies between about 0.5 and 40 Hz.
146 Plots of median PSD versus frequency shown in Figure 3 using the method of McNamara & Buland
147 (2004) show that some of the stations experience high noise levels, confirming the previous
148 analyses of Raspberry Shake hardware by Anthony et al. (2019) and Holmgren & Werner (2021).
149 These elevated levels in the range 1-40 Hz are likely due to a combination of sub-optimal
150 deployment locations and local anthropogenic noise.

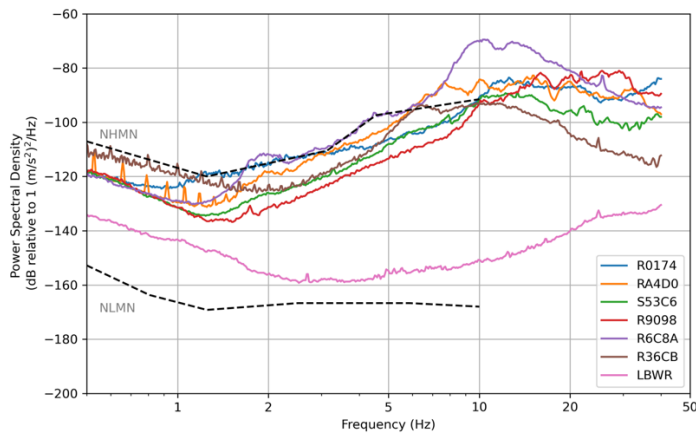
151



152

153 **Figure 2.** Frequency response of two Raspberry Shake stations used in this study. **a)** R6C8A is a 1D unit installed
 154 on Oxford Road in the city centre, with a vertical geophone only. **b)** R9098 is a 3D unit installed at Astley (semi-
 155 rural) with 2 horizontal and 1 vertical geophones.

156



157

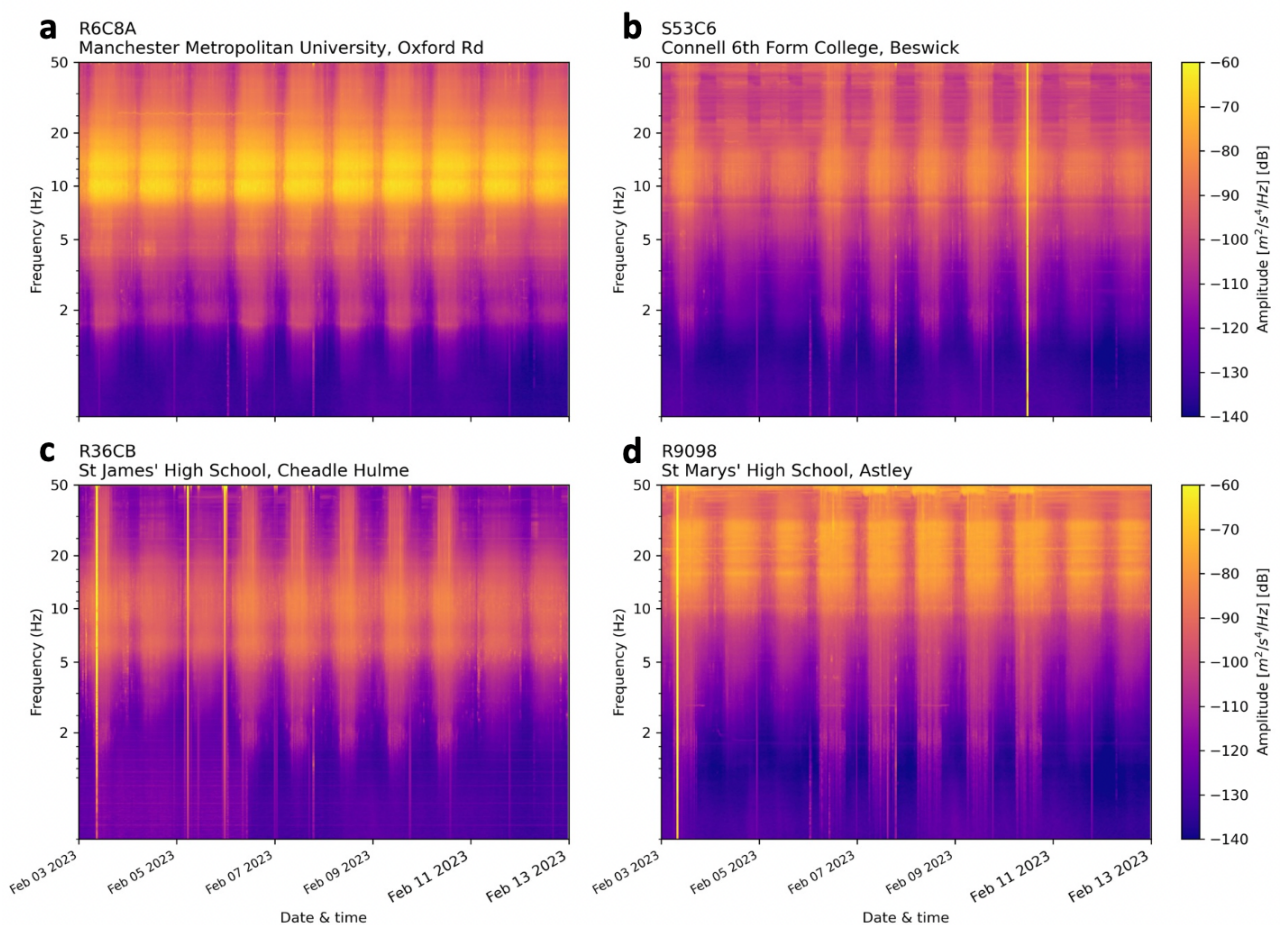
158 **Figure 3.** Plot showing vertical-component noise power spectral density (PSD) for stations used in this study over
 159 a single typical 24 hour period, and compared to that from the nearest British Geological Survey broadband
 160 station (LBWR) at Ladybower Reservoir in the Peak District, approximately 45 km ESE from Manchester city
 161 centre.

162

163 3. Results

164 3.1 Spatial and diurnal variations in vibrations across Greater Manchester

165 Vertical-component noise power varies significantly across Greater Manchester and over different
166 timescales (weeks, days, hours; see Figures 4 and 5). Noise is much higher (+20 dB), on average, in
167 city centre or urban locations compared to those sites in the outlying suburbs and semi-rural areas
168 on the edge of the conurbation (compare Figures 4a & b with Figures 4c & d, respectively). The
169 frequency band of the highest acceleration powers vary from site to site. In the city centre (station
170 R6C8A, Oxford Road), this frequency is quite well defined between 10 and 15 Hz, whereas in a
171 semi-rural location (R9098, Astley), it ranges from 10-30 Hz. At all sites, clear diurnal variations are
172 visible in the spectrograms (Figure 4), with reductions of about 20 dB from the middle of the day
173 to night time. The overall spread of frequencies is much larger during weekdays too, with ranges
174 from 2–50 Hz for weekdays compared to 5-30 Hz for weekends and holidays.
175



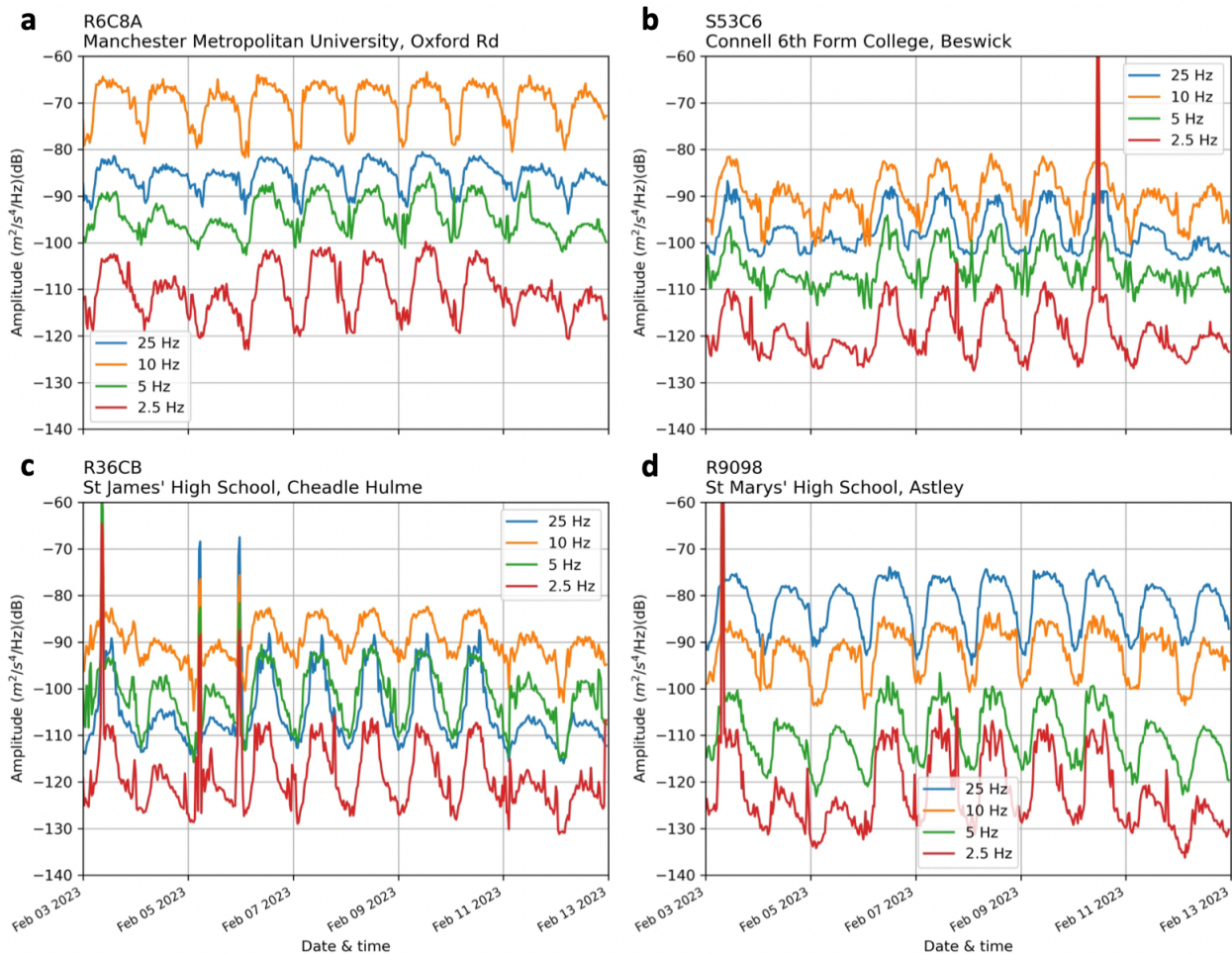
176

177 **Figure 4.** Spectrograms showing vertical-component noise PSD for the same 10-day period, including 2
178 weekends, for 4 different locations around Greater Manchester. **a)** R6C8A at Manchester Metropolitan
179 University on Oxford Road (city centre); **b)** S53C6 at Connell Co-op Academy in Beswick (urban); **c)** R36CB at St
180 James' Catholic High School in Cheadle Hulme (suburban); and **d)** R9098 at St Marys' Catholic High School in
181 Astley (semi-rural).

182

183 Figure 5 shows the amplitude of noise power for selected frequencies at the same four stations
184 shown in the spectrograms in Figure 4. The shape of the diurnal variations in noise is now more
185 apparent. Most sites show at least 10 dB variation in peak noise between day and night, except for
186 the city centre station R6C8A. The difference between peak noise on weekdays versus weekends,
187 at a given frequency, is of the order of 5-10 Hz. Interestingly, different sites show different shapes
188 i.e., gradients, of noise variation in time across each day. Some sites show a rapid morning rise in
189 noise, followed by slower drop to night-time levels (e.g., R6C8A and R9098), whereas others show
190 more symmetric rises and falls in the noise levels during the day (e.g., R36CB and S53C6). The
191 shapes of temporal variation in noise at a given frequency also vary from weekdays to weekends,
192 with weekend days generally being more symmetric over 24 hours compared to weekdays.

193



194

195 **Figure 5.** Plots of PSD at selected frequencies representing horizontal slices through the spectrograms shown for
 196 the 10-day periods shown in Figure 4, for the same stations.

197

198 3.2 Comparison to empirical traffic counts

199 a) Transport for Greater Manchester (TfGM) Drakewell traffic cameras

200 Traffic count data has been extracted from the manchester-i Urban Observatory, and then

201 compared to the same time intervals as the seismometer recordings (Figure 6). Data from the

202 Transport for Greater Manchester (TfGM) Drakewell cameras is categorised into different vehicle

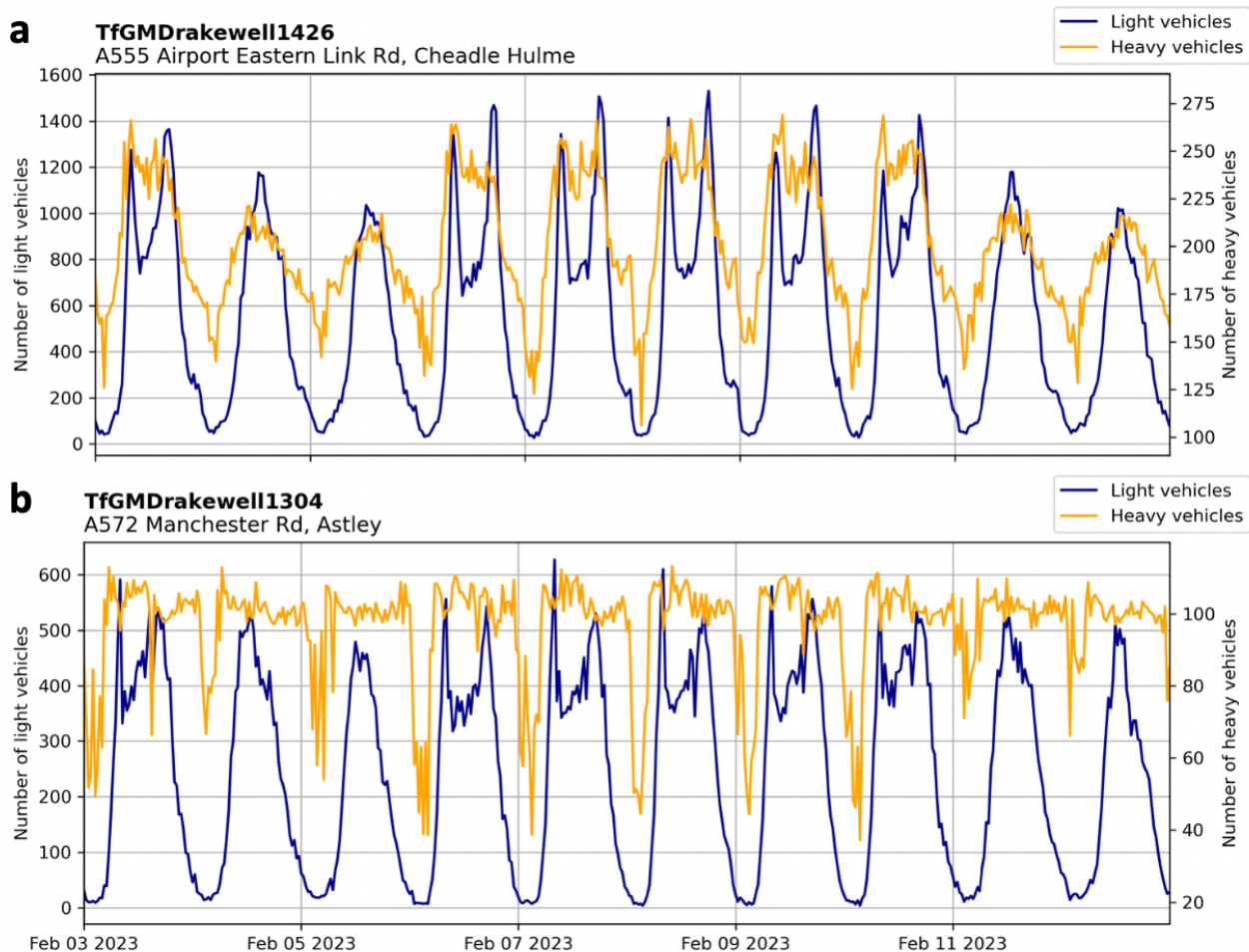
203 types, including cars, vans, buses & coaches and heavy lorries. For this study, I grouped the cars

204 and vans together as 'light vehicles' and the rest as 'heavy vehicles'. Figure 6 shows the temporal

205 variation in traffic counts at two sites close to stations R9098 at Astley and R36CB at Cheadle

206 Hulme for the same 10-day time interval as the seismic noise shown in Figures 4 and 5. The daily

207 rise and fall in traffic volume is apparent at both sites, although there are significant differences.
208 For camera 1426 at Cheadle Hulme (close to seismic station R36CB), the difference in shape and
209 size of weekends and weekdays is obvious, with broadly symmetric rises and falls of traffic volume
210 on each weekend day to a lower peak level, but a distinct double peak pattern on weekdays to
211 higher levels, with a steeper morning rise and more gradual evening drop-off. For camera 1304 at
212 Astley (close to seismic station R9098), the weekend peak counts are like those for weekdays,
213 although again the diurnal patterns are distinct, with double peak patterns on weekdays. At both
214 sites, the heavy vehicle traffic shows a steep morning rise and gradual fall through the afternoon
215 on each weekday.
216



217
218 **Figure 6.** Plots of traffic count time series from two Transport for Greater Manchester (TfGM) Drakewell cameras
219 located close to stations R36CB and R9098. Counts are shown for 30 minute bins across the same 10 day period

220 as the seismometer data in Figures 4 and 5. a) Drakewell camera 1426 close to seismometer R36CB in Cheadle
221 Hulme. b) Drakewell camera 1304 close to seismometer R9098 in Astley. See maps in Figure 1c-d for precise
222 locations.

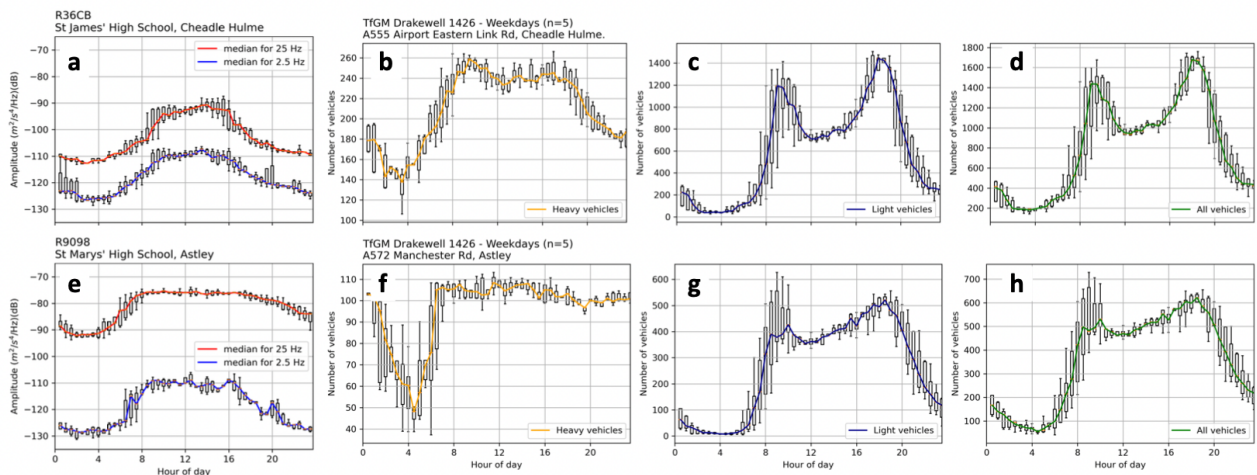
223

224 The similarity of the diurnal patterns observed in both the seismic noise and traffic count
225 data – including the changes in temporal gradients and the differences between weekdays and
226 weekdays – strongly suggests that traffic is the source for much of the seismic noise measured at
227 the nearest station. To investigate this apparent correspondence in more detail, Figure 7 shows
228 plots of noise amplitude at two selected frequencies (2.5 Hz and 25 Hz) for two stations. Following
229 Green et al., 2017 these data are plotted for five consecutive weekdays but wrapped around a 24
230 hour window, with the box and whisker format shows the statistical distribution in noise for each
231 half-hour interval. There are clear differences between the two sites, with station R9098 at Astley
232 showing much higher noise at 25 Hz than R36CB at Cheadle Hulme (for the same 5 day interval). In
233 addition the shape of the daily variation is different with a simple plateau at -75 dB for R9098
234 between 8 am and 5 pm, but a steadily rising curve to a peak of -90 dB at around 2 pm in Cheadle
235 Hulme. These patterns are repeated for the lower frequency of 2.5 Hz at both sites. Similar plots
236 for two consecutive weekends (giving 4 days total) at each site are shown in Figure N. By
237 comparison to the weekday intervals, the noise levels at weekends in these suburban locations are
238 clearly lower by about 5 – 15 dB for the same time of day. The distinctive plateau in the Astley
239 data for weekdays is absent at the weekends, replaced by a gently rising and falling curve. The gap
240 between the noise measured at 2.5 and 25 Hz for Astley is consistently 35-40 dB for weekdays and
241 weekends, whereas at Cheadle Hulme the gap is 10-15 dB.

242 The traffic count data from the closest Drakewell cameras to these two stations are plotted
243 in the same format in Figures 7c-d and 8c-d. The data are broken down into Heavy, Light and Total
244 vehicles and show the statistical distribution per half-hour time slot for the same intervals of

245 weekdays (Figure 7) and weekends (Figure 8). For Astley (camera 1304 and station R9098), the
 246 single plateau in the seismic noise is closely mirrored by the pattern for Heavy vehicles (buses,
 247 coaches, and lorries), but not for Light vehicles (cars, vans) which shows a double peak pattern
 248 corresponding to the morning and afternoon rush-hours. Similarly for Cheadle Hulme (camera
 249 1426 and station R36CB), the distinct double peak in the Light vehicle counts over 24 hours is not
 250 seen in the seismic noise for the same weekday period. For weekends, the traffic counts are
 251 slightly lower per half-hour interval, but the shape of the temporal variation over 24 hours is
 252 similar to that for weekdays for Heavy vehicles, but not for Light vehicles – the double peak (two
 253 rush-hour) pattern is now absent at weekends. From these data, I infer that the dominant
 254 contribution to the measured seismic noise between 2.5 and 25 Hz at both sites – on weekdays
 255 and weekends – probably comes from Heavy vehicles, with only a minor degree of modulation by
 256 the Light vehicle traffic.

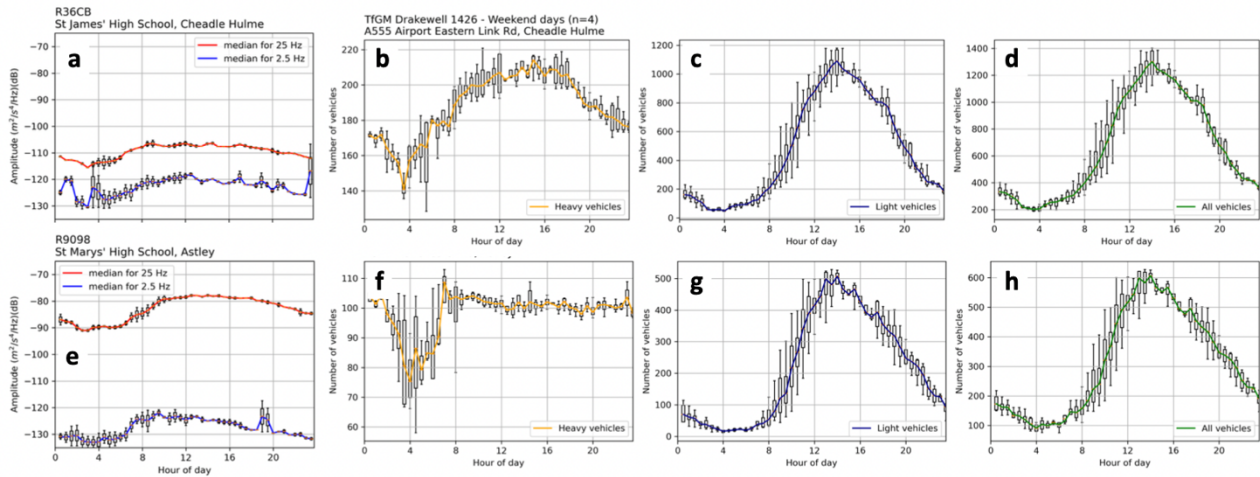
257



258

259 **Figure 7.** Plots of PSDs for selected frequencies for 5 consecutive weekdays at stations R36CB (Cheadle Hulme)
 260 and R9098 (Astley). The data are plotted in 'box and whisker' format to show the statistical distribution in 30
 261 minute bins across 24 hours in a day. The solid coloured lines show the median and the boxes span the 1st and
 262 3rd quartiles.

263



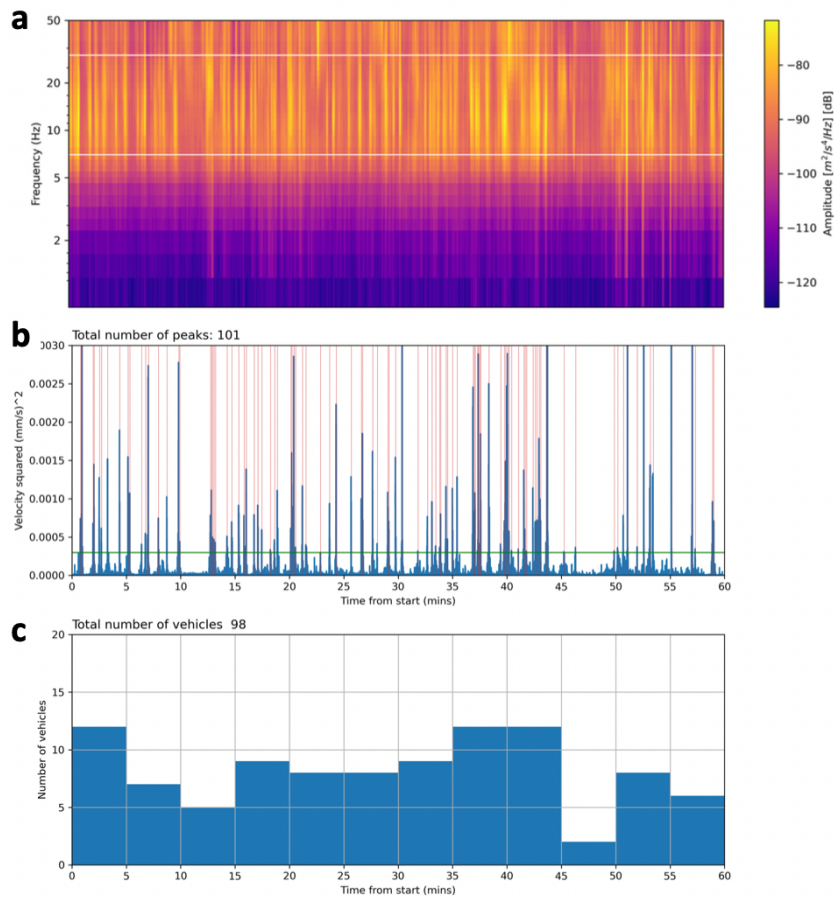
264

265 **Figure 8.** Plots of PSDs for selected frequencies for 2 consecutive weekends at stations R36CB (Cheadle Hulme)
 266 and R9098 (Astley). The data are plotted in 'box and whisker' format to show the statistical distribution in 30
 267 minute bins across 24 hours in a day. The solid coloured lines show the median and the boxes span the 1st and
 268 3rd quartiles.

269

270 *b) In-person traffic counts*

271 To further calibrate the potential for Raspberry Shake seismometers to quantify local traffic
 272 volumes, we ran comparisons between in-person traffic counts over 30-60 minute intervals
 273 outside two houses where seismometers were located in the Chorlton area of south Manchester.
 274 In-person traffic count data were collected by local volunteers at the roadside and binned at 5-
 275 minute intervals (Figure N). An example of the seismic noise is plotted in spectrogram format for
 276 frequencies between 1 and 50 Hz (Figure N). Short duration (up to a few seconds) high amplitude
 277 events are clear between about 5 to 35 Hz. A bandpass filter was applied to the raw seismometer
 278 data and the instrument response removed, before squaring the resulting velocity (Figure N).
 279 Applying a simple arbitrary threshold above the background to this plot shows a near perfect
 280 correspondence in peaks of velocity measured by the seismometer and the in-person counts (101
 281 recorded peaks versus 98 observed vehicles, respectively). In total, we ran four separate in-person
 282 counts (during morning and afternoon rush-hours) at each of the two Chorlton stations for a total
 283 of eight calibrations, with similar results for all.



285

286 **Figure 9.** Plots showing the calibration of a seismometer response to in-person traffic counts in Chorlton, south

287 Manchester. The data shown are from station RA4D0 located in a house on Claude Road. **a)** Spectrogram of

288 vertical-component noise PSD for a time window of 60 minutes in the morning of DD/MM/23. The raw data

289 have been high-pass filtered at 1 Hz. Note the regular high-amplitude events concentrated in the frequency

290 range 7-35 Hz. **b).** Vertical-component velocity² for the same time interval as a) and filtered between 7-35 Hz.

291 The number of peaks above an arbitrary threshold of 0.0003 mm^2/s^2 is 101. **c)** Bar chart of in-person vehicle

292 counts binned into 5 minute intervals for the same time interval as a) and b) conducted directly outside the

293 house containing seismometer RA4D0. The total number of road vehicles (excluding bicycles) is 98.

294

295 *3.3 Variations of seismic noise and traffic around School Streets road closures*

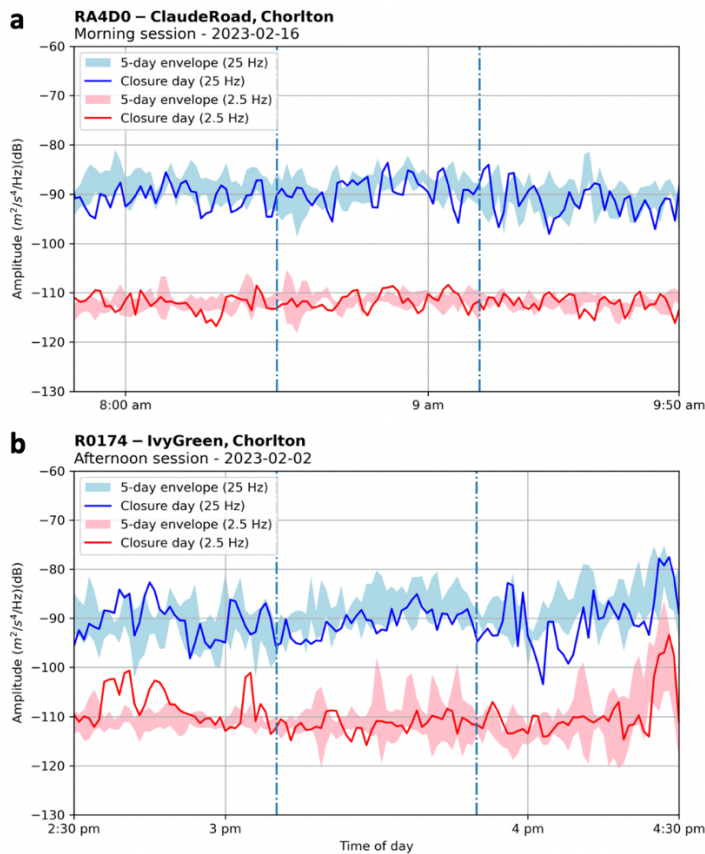
296 School Streets is a community-led initiative backed by local authorities in certain areas of the UK

297 (Chivers et al., 2019; ...). The road outside or close to a school is temporarily closed to traffic at

298 morning drop-off and afternoon pick-up times. The aims are to reduce air pollution and traffic

299 danger, and encourage active travel (walking, cycling) to and from school. In Chorlton, Brookburn
300 Primary school has been conducting School Streets pilot projects to assess the impact on local
301 traffic. On selected days, an approximately 150 m long section of Brookburn Road is closed to
302 through traffic between 08:30 and 09:10 and then again between 15:10 and 15:50. During
303 preliminary consultations with residents, concerns were expressed that traffic volumes may locally
304 *increase* at either end of the closed road section, due to cars turning around to avoid the closure.
305 To test this, we installed Raspberry Shake seismometers at either end of the closed section, close
306 to junctions where traffic might be expected to increase (map in Figure 1e). In addition to the in-
307 person traffic count calibrations, we measured a background seismic noise dataset from a full 5-
308 day school week with no road closures to serve as a reference level for any changes, at two
309 selected frequencies 25 and 2.5 Hz, shown as the shaded blue and red zones, respectively, in
310 Figure 10. These envelopes are defined by the minimum and maximum for each 1 minute interval
311 for the 5 days. The choice of two frequencies was based on the findings reported above that
312 different stations record traffic variations across a frequency band rather than one well-defined
313 frequency. Data for two separate road closures - one in the morning (Figure 10a) and one in the
314 afternoon (Figure 10b) – are shown in Figure 10, for two stations and two frequencies (blue and
315 red lines). The recorded noise levels sit well within the 5-day envelopes recorded for non-closure
316 days, supporting the inference that road closures are not currently leading to increased traffic
317 volumes at either end of the School Streets section. Over 6 road closure pilots so far, none have
318 shown any increase in noise attributable to road traffic before, during or after the School Streets
319 closure windows.

320



321

322 **Figure 10.** Plots of PSDs for selected frequencies (2.5 & 25 Hz) for School Streets closure periods in Chorlton.

323 Shaded zones show the range (min, max) recorded over a 5-day interval during which there were no road

324 closures to serve as a reference. **a)** Data measured at station RA4D0 on Claude Road at the eastern end of the

325 School Streets section. **b)** Data measured at station R0174 on Ivy Green Road at the western end of the section.

326 In both cases, the signals from the closure periods (solid lines) sit well within the background range (shaded

327 zones), and this is consistent across two frequencies and two separate sites.

328

329 **4. Discussion**

330 As reported by Green et al. (2017) for London, it is perhaps unsurprising that there is a good

331 correlation of seismically measured noise at certain frequencies with traffic volumes around

332 Greater Manchester, but there are some specific features that merit further analysis. One obvious

333 point is the geographic variation in noise levels measured by the Raspberry Shake seismometers in

334 this study, with sites ranging from urban city centre (e.g., R6C8A at Manchester Metropolitan

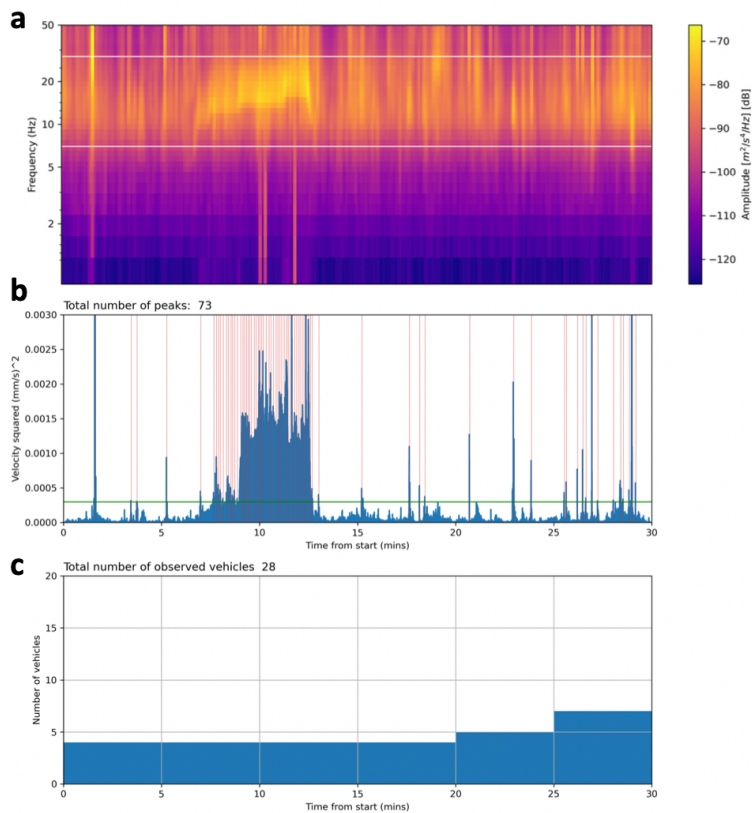
335 University, MMU) to semi-rural (R9098 at Astley). Peak amplitudes shown on the PSD

336 spectrograms vary between sites, and the shape of diurnal variations over 24 hours is also distinct.
337 Moreover, the diurnal patterns for weekdays are distinct from weekends and public holidays. The
338 availability of high quality digital traffic count data from the TfGM Drakewell project through the
339 manchester-l web portal enables the quantitative comparison of road traffic with seismic noise.
340 Note that there is no subway or underground train network in Manchester, but there are surface
341 trams (Metrolink) and overground rail lines. The seismometer closest to a railway line in this study
342 is the station at Oxford Road R6C98 (MMU) at approximately 400 metres. Future analysis of train
343 timetables in relation to the recorded data at R6C98 may explain the near constant (24/7) high
344 amplitude noise, noting that this line is used for passenger and freight traffic.

345 In comparison to other cities, the measured noise is comparable in terms of power
346 amplitudes and frequency ranges. Seismic noise from traffic in Bucharest (Romania) was measured
347 by Groos & Ritter (2009), and spanned 1-45 Hz with a peak between 1-10 Hz. Boese et al. (2015)
348 used borehole seismometers to measure ambient noise around rugby matches and railway lines in
349 Auckland (New Zealand). The noise from traffic peaked at 7 Hz, in a range spanning 1-35 Hz. Riahi
350 & Gerstoft (2015) used a dense geophone network to measure seismic noise from aircraft, trains
351 and road traffic in Long Beach, California (USA). They could track individual heavy goods vehicles
352 moving along highway 1-405 at night time, with a peak amplitude at between 10-20 Hz. Diurnal
353 variations in noise recorded in London (UK) by Green et al. (2017) peaked at about 90 dB at a
354 frequency range of 2.5 Hz (period = 0.4 s). Road traffic in Barcelona (Spain) measured by Diaz et al.
355 (2017) peaked at X dB in a range of 8-12 Hz. These previous studies used standard broadband
356 seismometers rather than citizen science Raspberry Shake seismometers.

357 In terms of other contributions to the measured noise, note that the any microseism
358 component is probably not relevant, as the data used in this study have been high-pass filtered at
359 1 Hz. In addition, site specific effects from varying bedrock geology may be significant, but could
360 only be achieved with 3-component stations to conduct HVSr analysis. The stations used in this

361 study were a mixture of 1- and 3-component Raspberry Shakes. A first target of this future analysis
362 would be to compare stations sited on Carboniferous Coal Measures with those on Permo-Triassic
363 sandstones. The siting of any seismometer is a key factor in the quality of the recorded data. Some
364 of the stations in this study were placed in sub-optimal locations – e.g., in domestic homes, not on
365 the ground floor, and not on a smooth stable concrete base. This can result in occasional
366 contributions to the data from non-road traffic. An example is shown in Figure 11 for station
367 R0174 used in the Chorlton School Streets project. The event happened during one of our in-
368 person traffic calibrations, with a volunteer counting cars outside the location of the seismometer.
369 An intense signal of rising frequency occurs at approximately 7 minutes into the 30 minute survey,
370 and lasts for about 7 minutes (spectrogram in Figure 11a). This signal dominates the recording and
371 obscures the shorter duration lower energy events from passing vehicles, and therefore renders
372 the simple peak-counting algorithm redundant in this case. Work-arounds include processing the
373 data to remove artefacts of this form, or asking the residents of the house with the seismometer
374 to schedule domestic appliances outside the time windows of the School Streets closures.
375



376

377

Figure 11. Plots showing the attempted calibration of a seismometer response to in-person traffic counts in

378

Chorlton, south Manchester. The data shown are from station R0174 located in a house on Ivy Green Road. **a)**

379

Spectrogram of vertical-component noise PSD for a time window of 30 minutes in the morning of DD/MM/23.

380

The raw data have been high-pass filtered at 1 Hz. Note the regular high-amplitude events concentrated in the

381

frequency range 7-35 Hz, and the rising frequency (5 to 20 Hz) event starting at about 6 minutes and lasting for

382

about 7 minutes. This is likely to be from a domestic electrical appliance, such as a washing machine. **b).** Vertical-

383

component velocity² for the same time interval as a) and filtered between 7-35 Hz. The number of peaks above

384

an arbitrary threshold of 0.0003 mm^2/s^2 is 73, but dominated by events in the time window 6-13 minutes,

385

coinciding with the rising frequency event in a). **c)** Bar chart of in-person vehicle counts binned into 5 minute

386

intervals for the same time interval as a) and b) conducted directly outside the house containing seismometer

387

R0174. The total number of road vehicles (excluding bicycles) is 28.

388

389

5. Summary

390

In this study, I used open data from a network of affordable citizen science Raspberry Shake

391

seismometers installed across Greater Manchester to show that road traffic in different areas

392 generates distinct and measurable signals (formerly ‘noise’) that can be correlated to changes in
393 traffic volumes. Diurnal variations in amplitude at frequencies from 2.5 to 25 Hz correlate directly
394 with time series of traffic counts from automatic traffic cameras, including the gradients of
395 increase and decrease at morning and evening rush-hours, respectively. Spatial variations show
396 much higher amplitudes in city centre locations (e.g., station R6C8A on Oxford Road) compared to
397 suburban locations (e.g., R9098 at Astley). Over shorter time-periods (30 minutes to 1 hour), the
398 seismometers can accurately record the passing of individual vehicles, as demonstrated by
399 comparison of Raspberry Shake data to in-person traffic counts. Based on these findings, I have
400 trialled the use of Raspberry Shake seismometers around a School Streets temporary road closure
401 program in Chorlton, and found no increase in road traffic noise before, during or after the closure
402 windows in the local area.

403 The data and analysis presented here shows that low-cost citizen science seismometers,
404 like the Raspberry Shake, can be used to quantify road traffic levels in urban and suburban
405 environments. While broadband instruments are needed to analyse the full spectrum of
406 anthropogenic noise in these locations, lower cost devices, such as the Raspberry Shake with a
407 limited frequency response, can still provide useful quantitative information. Moreover, their
408 lower unit cost can enable a dense deployment of many instruments in each area. In addition, the
409 availability of the raw seismological data through public servers (International Federation of Digital
410 Seismograph Networks, FDSN) and the anonymity of the method – compared to perceived risks
411 about using camera-based systems – both combine to increase transparency when communicating
412 the results to the wider public, e.g. in School Streets road closure trials.

413

414 **Acknowledgements**

415 Tiffany Chong and Layla Seibert at Brookburn PTA Active Travel are thanked for enabling the
416 deployments of stations for the School Streets pilot in Chorlton, and George Coombs (formerly at

417 Our Streets Chorlton) helped connect me with relevant groups across Greater Manchester. Thanks
418 to Chas Mead and Jo Phillips for hosting seismometers in their homes, and to Liz Saul, Lynda Styfek
419 and Stuart Blackadder at Transport for Greater Manchester (TfGM). Thanks also to Rachel Berman
420 at the Greater Manchester Combined Authority (GMCA), and Ettore Murabito at the Manchester
421 Urban Observatory for invaluable help in accessing the Drakewell traffic camera data from
422 manchester-i. The open source Python packages ObsPy and Matplotlib were used throughout.
423 Amy Gilligan (Aberdeen) and Dave Cornwell (Aberdeen) are thanked for discussion. Parts of this
424 work were funded from UKRI NERC awards under the Discipline Hopping and Discovery Science
425 (NE/T007826/1) schemes.

426

427 **Data & code availability**

428 The raw Raspberry Shake timeseries data used in this study are available on the standard public
429 FSDN servers – network, channel etc. The traffic camera data used in Figures M-N have been
430 downloaded from the Manchester Urban Observatory manchester-i portal at [https://manchester-](https://manchester-i.com/)
431 [i.com/](https://manchester-i.com/) and copies of the files of traffic camera counts are stored in .csv format on GitHub at
432 <https://github.com/DaveHealy-github/listen2manchester>. The Python code used to generate Figs
433 M-N is also on GitHub at <https://github.com/DaveHealy-github/listen2manchester>. A snapshot of
434 these data and code files has also been stored on Zenodo at DOI: 10.5281/zenodo.7970854 (taken
435 25 May 2023).

436

437 **Competing interests**

438 The author declares that he has no competing interests.

439

440 **References**

441 Anthony, R.E., Ringler, A.T., Wilson, D.C. and Wolin, E., 2019. Do low-cost seismographs perform
442 well enough for your network? An overview of laboratory tests and field observations of the OSOP
443 Raspberry Shake 4D. *Seismological Research Letters*, 90(1), pp.219-228. DOI: 10.1785/0220180251
444

445 Beyreuther, M., Barsch, R., Krischer, L., Megies, T., Behr, Y. and Wassermann, J., 2010. ObsPy: A
446 Python toolbox for seismology. *Seismological Research Letters*, 81(3), pp.530-533. DOI:
447 10.1785/gssrl.81.3.530
448

449 Boese, C.M., Wotherspoon, L., Alvarez, M. and Malin, P., 2015. Analysis of anthropogenic and
450 natural noise from multilevel borehole seismometers in an urban environment, Auckland, New
451 Zealand. *Bulletin of the seismological Society of America*, 105(1), pp.285-299. DOI:
452 10.1785/0120130288
453

454 Chivers, H., Wong, A. and Preston, J., 2019. School streets case studies from Southampton-how
455 using temporary street closures and trial interventions can help to gain support for permanent
456 changes to improve our school environments. <https://eprints.soton.ac.uk/437850/>. Last accessed:
457 29 May 2023.
458

459 Department for Business, Energy and Industrial Strategy (UK government), 2021.
460 [https://www.gov.uk/government/statistics/uk-local-authority-and-regional-carbon-dioxide-](https://www.gov.uk/government/statistics/uk-local-authority-and-regional-carbon-dioxide-emissions-national-statistics-2005-to-2019)
461 [emissions-national-statistics-2005-to-2019](https://www.gov.uk/government/statistics/uk-local-authority-and-regional-carbon-dioxide-emissions-national-statistics-2005-to-2019). Last accessed: 25 May 2023.
462

463 Denton, P., Fishwick, S., Lane, V. and Daly, D., 2018. Football quakes as a tool for student
464 engagement. *Seismological Research Letters*, 89(5), pp.1902-1907. DOI: 10.1785/0220180078
465

466 Díaz, J., Ruiz, M., Sánchez-Pastor, P.S. and Romero, P., 2017. Urban seismology: On the origin of
467 earth vibrations within a city. *Scientific reports*, 7(1), p.15296. DOI: 10.1038/s41598-017-15499-y

468

469 Diaz, J., Ruiz, M. and Jara, J.A., 2021. Seismic monitoring of urban activity in Barcelona during the
470 COVID-19 lockdown. *Solid Earth*, 12(3), pp.725-739. DOI: 10.5194/se-12-725-2021

471

472 Green, D.N., Bastow, I.D., Dashwood, B. and Nippres, S.E., 2017. Characterizing broadband
473 seismic noise in Central London. *Seismological Research Letters*, 88(1), pp.113-124. DOI:

474 10.1785/0220160128

475

476 Holmgren, J.M. and Werner, M.J., 2021. Raspberry Shake Instruments Provide Initial Ground-
477 Motion Assessment of the Induced Seismicity at the United Downs Deep Geothermal Power
478 Project in Cornwall, United Kingdom. *The Seismic Record*, 1(1), pp.27-34. DOI:

479 10.1785/0320210010

480

481 IPCC, 2021: Summary for Policymakers. In: *Climate Change 2021: The Physical Science Basis.*

482 *Contribution of Working Group I to the Sixth Assessment Report of the Intergovernmental Panel*
483 *on Climate Change* [Masson-Delmotte, V., P. Zhai, A. Pirani, S.L. Connors, C. Péan, S. Berger, N.

484 Caud, Y. Chen, L. Goldfarb, M.I. Gomis, M. Huang, K. Leitzell, E. Lonnoy, J.B.R. Matthews, T.K.

485 Maycock, T. Waterfield, O. Yelekçi, R. Yu, and B. Zhou (eds.)]. Cambridge University Press,

486 Cambridge, United Kingdom and New York, NY, USA, pp. 3–32, DOI: 10.1017/9781009157896.001

487

488 Lecocq, T., Hicks, S.P., Van Noten, K., Van Wijk, K., Koelemeijer, P., De Plaen, R.S., Massin, F.,

489 Hillers, G., Anthony, R.E., Apoloner, M.T. and Arroyo-Solórzano, M., 2020. Global quieting of high-

490 frequency seismic noise due to COVID-19 pandemic lockdown measures. *Science*, 369(6509),
491 pp.1338-1343. DOI: 10.1126/science.abd2438

492

493 McNamara, D.E. and Buland, R.P., 2004. Ambient noise levels in the continental United States.
494 *Bulletin of the seismological society of America*, 94(4), pp.1517-1527. DOI: 10.1785/012003001

495

496 Office for National Statistics, 2023. <https://www.ons.gov.uk/visualisations/areas/E11000001/>. Last
497 accessed: 25 May 2023.

498

499 Peterson, J., 1993. Observations and modeling of seismic background noise. (Vol. 93, pp. 1-95).
500 Reston, VA, USA: US Geological Survey. DOI: 10.3133/ofr93322

501

502 Plant, J A, Jones, D G, and Haslam, H W (editors). 1999. *The Cheshire Basin: Basin evolution, fluid*
503 *movement and mineral resources in a Permo-Triassic rift setting*. (Keyworth, Nottingham: the
504 British Geological Survey). ISBN 0 85272 333 4

505

506 Riahi, N. and Gerstoft, P., 2015. The seismic traffic footprint: Tracking trains, aircraft, and cars
507 seismically. *Geophysical Research Letters*, 42(8), pp.2674-2681. DOI: 10.1002/2015GL063558

508

509 Walker, A., Baptie, B. and Ottemoller, L., 2003. UK earthquake monitoring 2002/2003.
510 <https://nora.nerc.ac.uk/id/eprint/527566>. Last accessed: 25 May 2023.